Toward All Aerosol Printing of High-Efficiency Organic Solar Cells Using Environmentally-friendly Solvents in Ambient Air

Ping Yang[1,2 #], *Tianqi Zhai*[2 #], *Boyang Yu*[2], *Gengxin Du*[2], *Baoxiu Mi*[1*], *Xinyan Zhao*[2,3*], *Weiwei Deng*[2,*]

1. Institute of Advanced Materials (IAM), Key Laboratory for Organic Electronics & Information Displays (KLOEID), Nanjing University of Posts & Telecommunications (NUPT), Nanjing 210023, China

2. Department of Mechanics and Aerospace Engineering, Southern University of Science and Technology (SUSTech), Shenzhen 518055, China

3. Academy for Advanced Interdisciplinary Studies, Southern University of Science and Technology (SUSTech), Shenzhen 518055, China

KEYWORDS: Organic solar cells, aerosol printing, scalable fabrication, green solvent

#: These authors contributed equally.

The operational principle and droplet size of ultrasonic spray

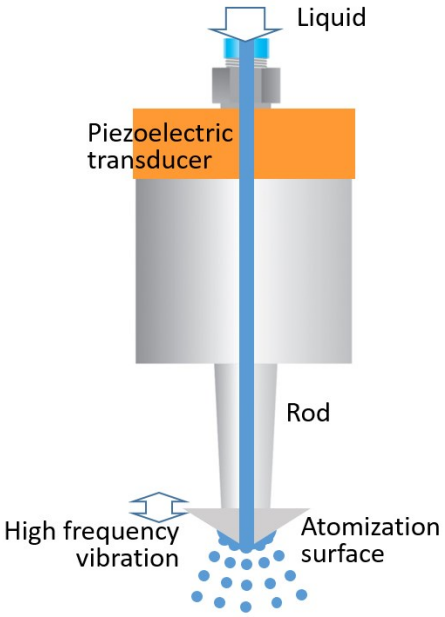

Figure S1 The schematic of the ultrasonic spray

For an ultrasonic spray, the liquid solution is fed through a hollow rod and spread on a conical or flat atomization surface (Figure S1). The rod is driven by a high power (on the order of ~100 Watt) piezoelectric transducer at a typical frequency of 40 kHz. The vibration of the rod induces Faraday waves on the liquid layer, and the wavelength [1] is $\lambda = (8\pi\sigma / \rho f^2)^{1/3}$, which is ~100 μm for typical parameters. Here σ is the liquid surface tension, ρ is the liquid mass density, and f is the frequency of the transducer. Ultrasonic spray is robust and the generated droplets are quite uniform. However, the droplet size is estimated by $d_0 \approx 0.4\lambda \sim 40$ μm, which appears to be too large for making uniform thin film of the photoactive layer (~100 nm thick) and hole/electron transport layer (10 to 40 nm thick) of OSCs, unless a very dilute solution is used.

Impactor model

The deposition of an aerosol jet can be modeled by the impactor model [2].

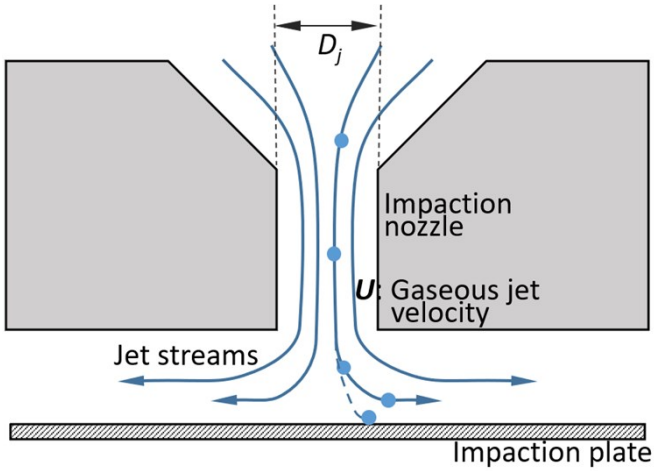

Figure S2 Cross-sectional view of an impactor

Take the nozzle in Figure S9 for example. The gas stream passes through the narrow nozzle at a velocity U. When an obstacle (i.e. impaction plate, or the ITO substrate) is in front of the stream, the stream can easily make a turn to avoid the obstacle. However, droplets with sufficient inertia in the stream will deviate from the gas stream, and they will impact on the plate.

The key parameter that governs the deposition (or collection) efficiency is the Stokes number, which is defined as the ratio of the stopping distance of droplet with velocity U to the aerosol jet half-width $D_j/2$:

$$S_{tk} = \frac{\tau}{D_j/(2U)}. \quad (1)$$

Here the slit (or a narrow rectangle) nozzle produces a two-dimensional aerosol jet of width D_j and length L. The stopping time of the droplet is: $\tau = m/(3\pi\mu_g d) = \rho_d \pi d^2/18\mu_g$,

where m is the droplet mass, d is the droplet diameter, ρ_d is the mass density of the droplet, and μ_g is the gas viscosity. Therefore, Equation 1 becomes

$$S_{tk} = \frac{\rho_d d^2 U}{9\mu_g D_j}. \quad (2)$$

The velocity of the aerosol stream is $U=Q_{gas}/(D_j L)$. The relationship between Stokes number and the carrier gas flow rate at different nozzle widths.

The impaction efficiency is a function of the Stokes number, and it increases as Stk increases. To achieve >50% deposition for the rectangle nozzle, the minimum Stokes number should be $S_{tk} \geq 0.59$.

Experimental Section

Materials: Unless stated otherwise solvents and chemicals were obtained commercially and used without further purification. PTQ10 and PDINO were purchased from 1 Material. Y6-BO was purchased from Derthon Optoelectronic Materials Science & Technology. The PEDOT:PSS (CLEVIOS P VP AI4083, Heraeus) was purchased from Ossila. The Chloroform (CF) (analytical grade) was purchased from Sigma Aldrich Co.

Vibrating meshes atomization (VMA): The VMA used in this work has ~450 micro-orifices, whose diameters range from 6~8 μm. The array of the orifices occupies 8.58 mm^2 area of the foil. The distance between the two neighboring holes is 127 μm. The resonance frequency of this VMA is 160 kHz. The droplet size distribution of the aerosol generated by VMA is characterized by a spray analyzer (Malvern Spraytec) based on laser scattering principles. The average diameter is at 5 μm, and the relative standard deviation (RSD) is 30%.

Aerosol printing of the functional layers: PEDOT:PSS: ethanol: DI water solution was prepared with a volume ratio of 2:7:1 and the solution was ultrasonically agitated for 30 mins. The PEDOT:PSS layer was printed by the VMA with carrier gas (N_2) flow rate of 3

L/min, liquid flow rate of 280 μl/min, atomization frequency of 160 kHz, and stage motion velocity of 3 mm/s. Under these conditions, the printed thickness of the PEDOT:PSS layer was ~40 nm. Then the PEDOT:PSS layer was annealed at 150 °C for 10 mins. PTQ10:Y6-BO (1:1.2 by weight) solution was prepared in O-XY (8 mg/mL). The solution was stirred for 8 hours at 80 °C in the glovebox. The active layer was printed by the VMA with carrier gas (N_2) flow rate (Q_{gas}) of 2 L/min, liquid flow rate (Q_l) of 75 μl/min, atomization frequency of 160 kHz, and stage motion velocity of 3 mm/s. The syringe containing the active layer solution was heated at 80 °C by wrapping a heating foil. Under these conditions, the printed thickness of the active layer was ~100 nm. After preparation, the active layer was thermally annealed at 100 °C for 10 min. The PDINO solution was prepared in ethanol with the concentration of 0.5 mg/mL. The PDINO layer was printed by the VMA with carrier gas (N_2) flow rate (Q_{gas}) of 1.5 L/min, liquid flow rate (Q_l) of 260 μl/min, atomization frequency of 160 kHz, and stage motion velocity of 3 mm/s. Under these conditions, the printed thickness of the PDINO layer was ~10 nm.

Fabrication of OSC devices: The organic solar cells studied in this work were fabricated with a structure of ITO/PEDOT:PSS/PTQ10:Y6-BO/PDINO/Ag. The ITO substrates were pre-cleaned in an ultrasonic bath of detergent, deionized water, acetone, and isopropanol for 15 mins and then were dried in a baking oven at 80 °C overnight. All ITO substrates were UV-treated in UV Ozone Cleaner (Ossila) for 15 mins. For the spin-coated solar cells, the PEDOT:PSS solution filtered through a 0.22 μm poly(ether sulfone) (PES) filter. A thin layer of PEDOT:PSS was deposited through spin-coating at 3000 rpm for 30 s on the ITO substrate. Then the PEDOT:PSS film was annealed at 150 °C for 10 mins in air. The active layer solutions were prepared at the concentration of 12 mg/ml (PTQ10:Y6-BO = 1:1.2) in chloroform (CF) and o-xylene (O-XY), respectively. The CF solution was stirred for 8 hours at room temperature and the O-XY solution was stirred for 8 hours at 80 °C. Then the solution was spin coated at 1500 rpm for 30 s onto the PEDOT:PSS layer. The active layer (ca. 100 nm) was thermal annealed at 100 °C for 10 min. PDINO solution was prepared in ethanol at concentration of 1 mg/mL and spin coated on the top of all the active layers at 3000 rpm for 30 s. For aerosol-printed solar cells, the active layer or all three

layers (PEDOT:PSS, active layer, PDINO) were fabricated by aerosol printing with parameters mentioned above. Finally, 100 nm Ag was evaporated through a shadow mask in a vacuum chamber at a pressure of 2×10^{-4} Pa, with an active area of 0.045 cm^2 and 1 cm^2.

Hole-only and electron-only devices: The hole-only devices have the architectures of ITO/PEDOT:PSS/PTQ10:Y6-BO/MoO_3/Ag, and the electron-only devices have the architectures of ITO/ZnO/PTQ10:Y6-BO/PDINO/Ag. For the electron-only devices, the ZnO precursor was prepared by dissolving 1 g zinc acetate dihydrate and 0.28 g ethanolamine in 10 ml 2-methoxyethanol under vigorous stirring for 12 h for the hydrolysis reaction in air. A 40 nm ZnO layer was spin-coated from the precursor solution on top of the clean ITO-glass substrate at 3000 rpm for 30 s, and annealed at 200 ℃ for 30 min in air. The active layers were deposited on the PEDOT:PSS or ZnO layers by spin coating or aerosol printing following the same procedures above. For the hole-only devices, 10 nm MoO_3 and 100 nm Ag were deposited in the vacuum of 2×10^{-4} Pa on the active layer.

Characterization: The current density-voltage (*J-V*) curves were characterized by a Keithley 2400 source meter under AM 1.5G illumination (100 mW cm^{-2}) with a class AAA solar simulator (Enlitech). Before each test, the solar simulator was calibrated by a NIST traceable reference single-crystal Si cell (Enlitech). The thicknesses of the thin films were measured using the AFM. The external quantum efficiency (EQE) spectra were recorded on a commercial EQE measurement system (QE-R3011, Enlitech). The SEM images were obtained by the scanning electron microscope (TM4000, Hitachi). The atomic force microscope (AFM) (XE7, Park System Inc.) was used for the surface morphological investigations. Transmission electron microscopy (TEM, Tecnai F30) was carried out using 300 kV. The active layer films for the TEM measurements were prepared by spin coating or aerosol printing on ITO/PEDOT:PSS substrates, and the substrates with active layers were submerged in deionized water to make the active layers float onto the air-water interface, then the floated films were picked up by copper grids. The absorption spectra of

the active films were measured using a UV-vis Spectrometer (UV-8000S, METASH). Grazing-incidence wide-angle X-ray scattering (GIWAXS) measurements were performed on Xeuss 2.0 (Xenocs). For our experiments, the light source was Cu Kα X-ray with wavelength of 1.54 Å (8.04 keV) and the grazing incident angle was 0.2°. All images were collected at a sample to detector distance of 161 mm and an exposure time of 45 min. Carrier mobilities were measured using the space charge limited current (SCLC) method using hole-only and electron-only diodes. The mobilities were obtained by fitting the current–voltage curves to a space charge limited current using the Mott-Gurney relationship.

Table S1 Fitting parameters of 1D GISAXS profiles of the spin coated and aerosol printed PTQ10:Y6-BO films.

Processing Methods	ζ (nm)	D (nm)	η (nm)	$2R_g$ (nm)
Aerosol printing	4.05	2.68	7.82	34.73
Spin coating	5.42	2.73	6.75	30.46

The domain size was quantified by fitting 1D GISAXS profiles and the fitting parameters are summarized in Table S1, where D is the fractal dimension of acceptor domains, ζ and η are the average correlation lengths of the donor-rich phase and acceptor-rich phase, respectively. The average domain size of the acceptor phase could be characterized by the size of clustered acceptor aggregates $2R_g$, which is calculated by the Guinier radius $R_g = \sqrt{\frac{D(D+1)}{2}}\eta$.

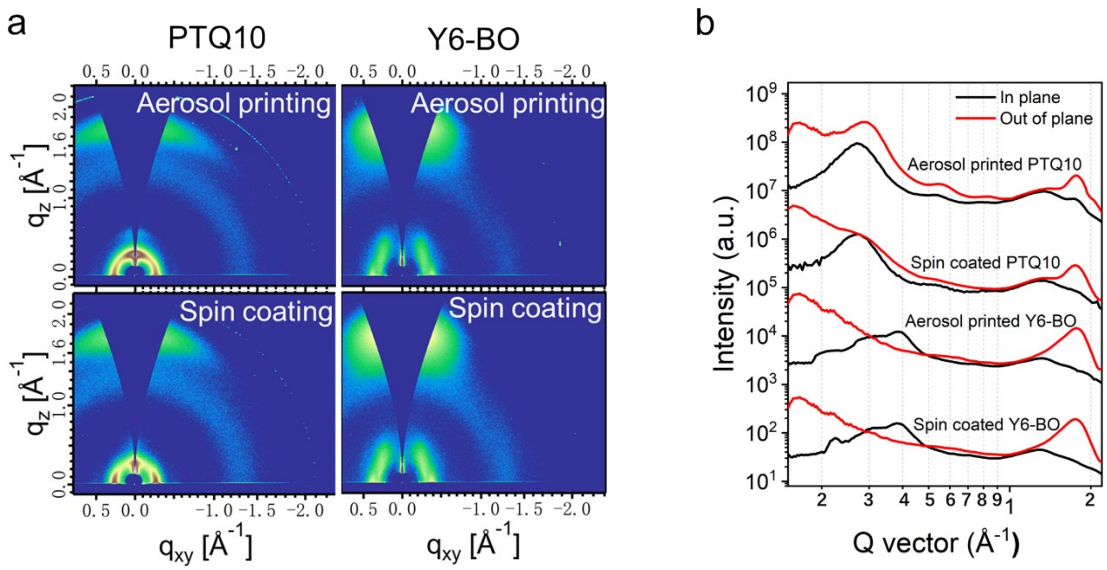

Figure S3 (a) Two-dimensional (2D) GIWAXS maps and (b) GIWAXS line cuts of neat PTQ10 film and neat Y6-BO film fabricated by aerosol printing and spin coating.

Table S2 Morphology parameters by fitting the out-of-plane and in-plane profiles from GIWAXS of blended PTQ10:Y6-BO, neat PTQ10 and neat Y6-BO films.

		Out of plane (010)			In plane (100)		
		Peak location (Å^{-1})	d-spacing (Å)	CCL (Å)	Peak location (Å^{-1})	d-spacing (Å)	CCL (Å)
PTQ10:Y6-BO	Aerosol printing	1.78	3.52	25.63	0.28	22.43	83.98
	Spin coating	1.75	3.59	25.89	0.28	22.43	78.16
PTQ10	Aerosol printing	1.75	3.59	29.16	0.27	23.09	97.58
	Spin coating	1.75	3.59	24.33	0.27	23.09	95.86
Y6-BO	Aerosol printing	1.78	3.35	26.38	0.38	16.53	53.32
	Spin coating	1.76	3.57	21.59	0.38	16.53	57.45

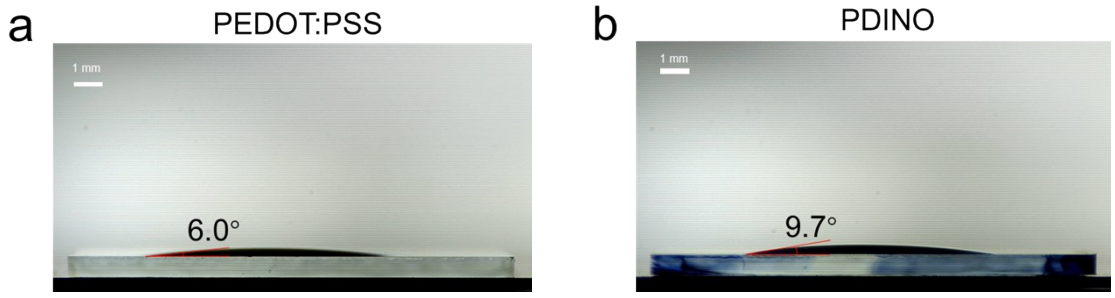

Figure S4 Contact angles of (a) PEDOT:PSS on ITO surface, and (b) PDINO on PTQ10:Y6-BO film.

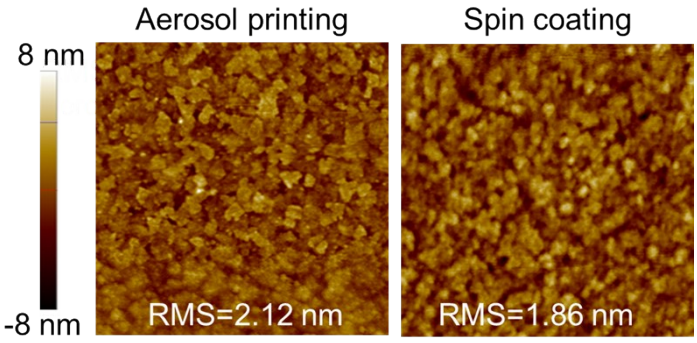

Figure S5 AFM surface topographic images (size: 5×5 μm^2) of aerosol-printed and spin-coated PEDOT:PSS films.

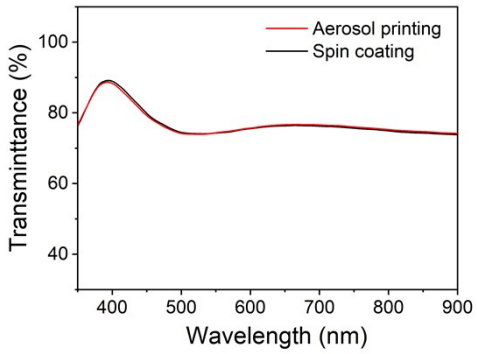

Figure S6 UV-vis absorption spectra of aerosol-printed and spin-coated PEDOT:PSS films.

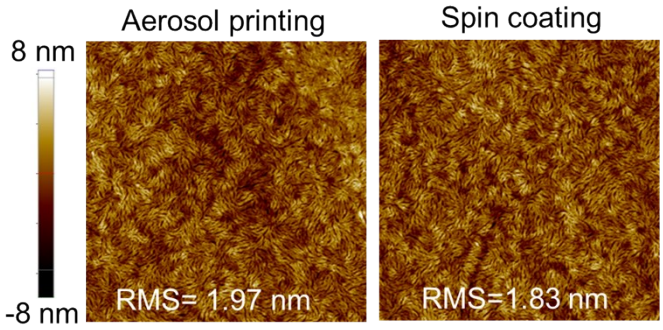

Figure S7 AFM surface topographic images (size: 5×5 μm^2) of aerosol-printed and spin-coated PDINO films.

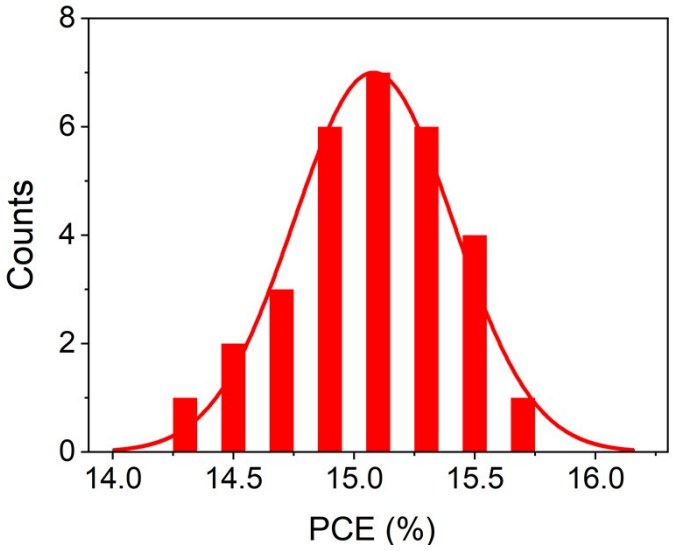

Figure S8 Histogram of OSCs (30 devices) based on PTQ10:Y6-BO prepared by aerosol printing.

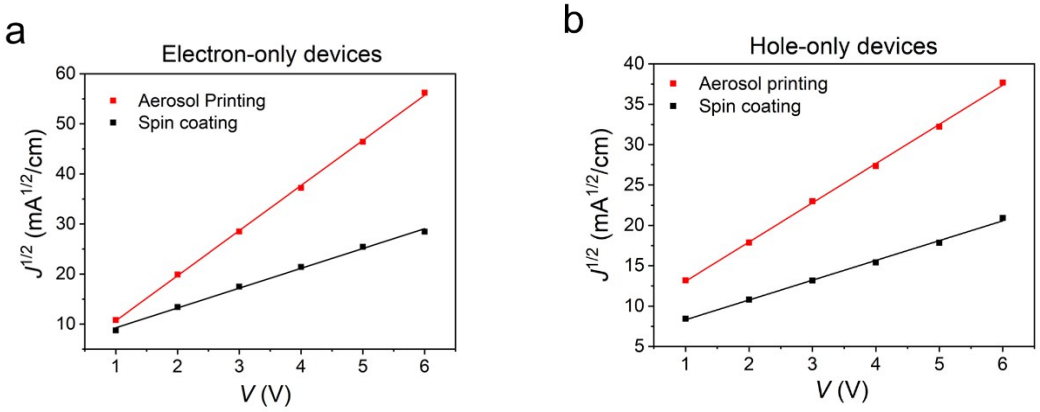

Figure S9 The $J^{1/2}$-V curves of the (a) electron-only devices and (b) hole-only devices calculated from the space charge limited current (SCLC) method of PTQ10:Y6-BO films prepared by aerosol printing and spin coating.

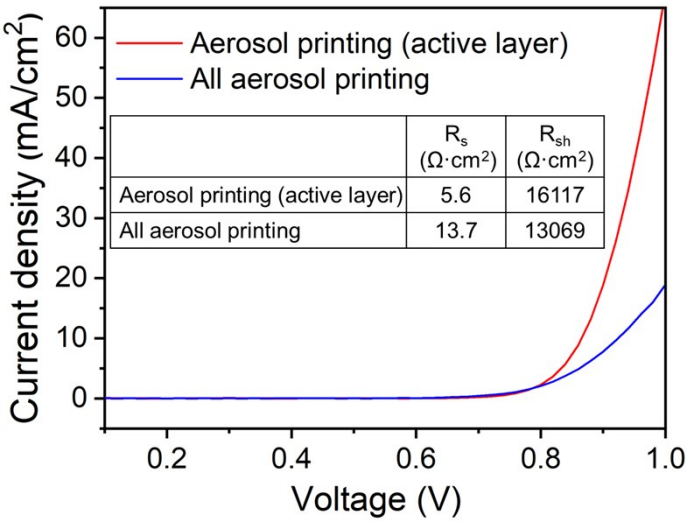

	R_s ($\Omega \cdot cm^2$)	R_{sh} ($\Omega \cdot cm^2$)
Aerosol printing (active layer)	5.6	16117
All aerosol printing	13.7	13069

Figure S10 The dark J-V curves of the device with aerosol-printed active layer and the all-aerosol-printed device. The shunt and series resistances are presented in the insert table.

Table S3. Comparison of performances of the reported OSCs printed by various droplet-based printing methods.

Methods	Printed layers	Active materials	Best PCE (%)	Refs	Years
Ultrasonic spray	Active layer	P3HT:PCBM	3.20	[55]	2009
		P3HT:PCBM	4.10	[56]	2011
		P3HT:PCBM	4.10	[57]	2013
		PBTI3T: $PC_{70}BM$	6.63	[58]	2016
		P3HT:PCBM	3.65	[59]	2016
		P3HT:PCBM	3.70	[60]	2016
		PBDTTT-EFT:$PC_{71}BM$	8.75	[18]	2016
		PTB7:$PC_{71}BM$	8.23	[16]	2018
		PTB7:$PC_{71}BM$	6.48	[15]*	2019
		PBDB-T:IT-M	8.06		
		PBDB-T-2Cl:IT-4F	12.29	[14]	2020
	Active layer & HTL	PCDTBT:$PC_{71}BM$	4.90	[61]	2015
		PBDTTT-EFT:$PC_{71}BM$	8.06	[18]	2016
		P3HT:PCBM	1.54	[62]	2017
Pneumatic spray	Active layer	P3HT:$PC_{61}BM$	2.35	[71]	2008
		TQ1:$PC_{61}BM$	3.90	[17]	2017
		PTB7:P(NDI2OD-T2)	7.07	[64]	2017
	Active layer & HTL& ETL	P3HT:PCBM	3.17	[65]	2012
Electrospray	Active layer	P3HT:$PC_{61}BM$	3.25	[66]	2010
		P3HT:$PC_{61}BM$	2.17	[67]	2012
		P3HT:$PC_{61}BM$	2.99	[23]	2014
		P3HT:$PC_{61}BM$	3.09	[22]	2015
		PTB7:$PC_{71}BM$	5.60	[68]	2017
		PTB7-Th:$PC_{71}BM$	8.60	[69]	2017
		P3HT:$PC_{61}BM$	4.20	[21]	2018
		PTB7-Th:FOIC	9.45	[20]	2020
	Active layer & HTL	P3HT:$PC_{61}BM$	3.08	[70]	2012
	Active layer & HTL& ETL	PTB7-Th:FOIC	8.71	[20]	2020

Inkjet Printing	Active layer	P3HT:$PC_{61}BM$	1.40	[71]	2008
		PCPDTBT:$PC_{61}BM$	1.48	[72]	2011
		PCDTBT:$PC_{70}BM$	3.86	[73]	2014
		Si-PCPDTBT:$PC_{70}BM$	3.01		
		P3HT:O-IDTBR	6.47	[13]	2019
	Active layer & HTL	P3HT:$PC_{61}BM$	3.71	[74]	2010
		PCDTBT:$PC_{70}BM$	5.05	[12]	2014
		P3HT:PC60BM	2.20	[75]	2015
Aerosol Jet Printing	Active layer	P_3HT:$PC_{60}BM$	2.53	[27]	2011
		PCBTDPP:$PC_{70}BM$	3.92		
Aerosol Printing	Active layer	PTQ10:Y6-BO	14.78	This work	2021
	Active layer & HTL& ETL	PTQ10:Y6-BO	15.65		

*An ultrathin pneumatic-sprayed active layer stacked on top of the thick ultrasonic-sprayed active layer.

References

[1] R. J. Lang, Ultrasonic Atomization of Liquids, *The Journal of the Acoustical Society of America* **34**, 6 (1962); doi: 10.1121/1.190902

[2] W. C. Hinds, Aerosol Technology: Properties, Behavior, and Measurement of Airborne Particles, 2nd Edition, Wiley, New York 1999.